Bottlenecks to vibrational energy flow in OCS

Structures and mechanisms

R. Paškauskas[1] C. Chandre[2] T. Uzer[3]

[1]Sincrotrone Trieste (ELETTRA), Trieste, Italy
[2]Centre de Physique Théorique CNRS, Marseille, France
[3]Georgia Institute of Technology, Atlanta GA, U.S.A.

Workshop on Stability and Instability in Mechanical Systems:
Applications and Numerical Tools
Barcelona, 1–5 December 2008

Outline of the talk

1. Observations and Phenomenology of Energy Transfer Processes
   - Transfer of Energy in Small Molecules
   - Chaotic transport: Hydrogen in Crossed Fields
   - Summary
2. Focus: Invariant Tori in the Phase Space of OCS
   - Tools to Detect Resonances
   - Unstable Tori as Transition Bottlenecks
   - Geometry of Invariant Surfaces

Outline of the talk

The OCS molecule
Introduction

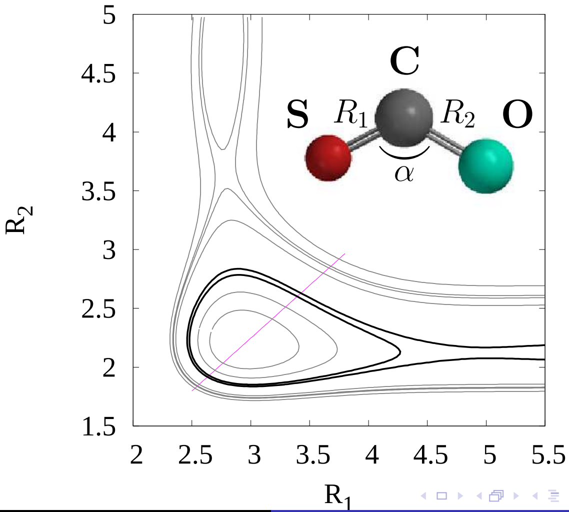

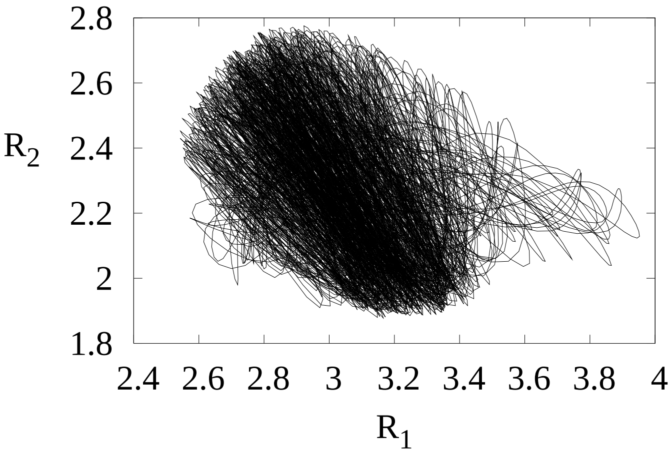
2.8
2.6
2.4
2.2
2
1.8
R_2
2.4 2.6 2.8 3 3.2 3.4 3.6 3.8 4
R_1

Obervations: Chaotic Trajectories

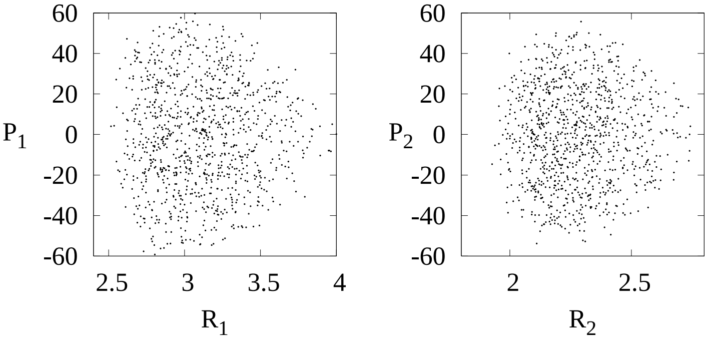

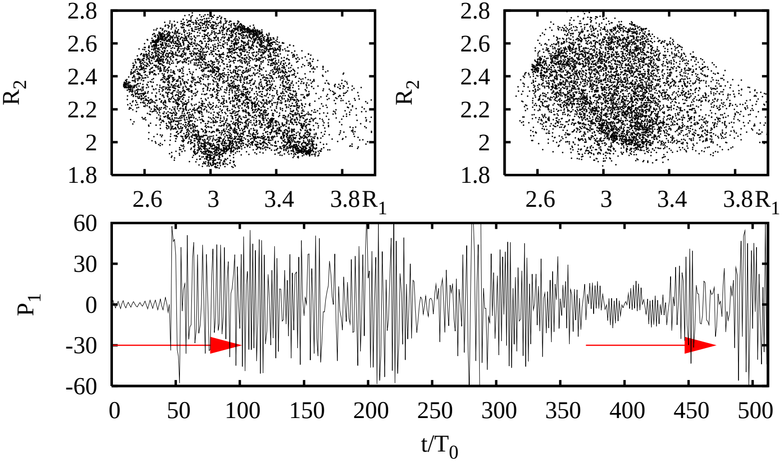
2.8
2.6
2.4
2.2
2
1.8
R_2
2.6
3
3.4
3.8
R_1
60
30
0
-30
-60
P_1
0
50
100
150
200
250
300
350
400
450
500
t/T_0

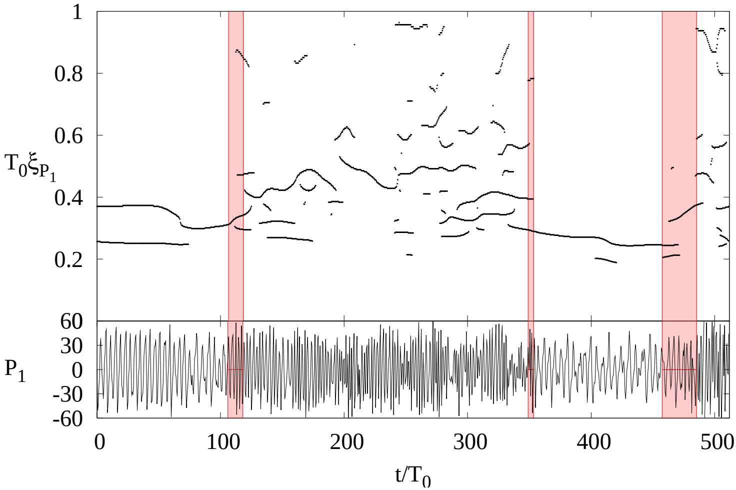
1
0.8
0.6
0.4
0.2
$T_0\xi_{P_1}$
60
30
0
-30
-60
P_1
0
100
200
300
400
500
t/T_0

Phenomenology of OCS

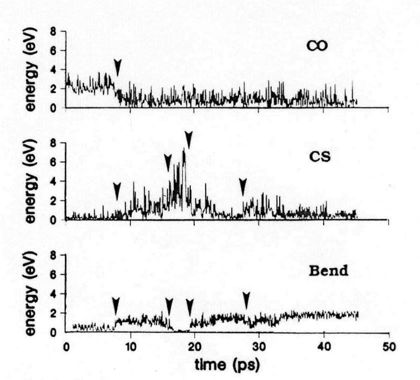

FIG. 1: Time dependence of normal mode energies for a planar OCS trajectory at an energy of 20,00 cm^{-1}. The labels CO, CS and Bend indicate the internal coordinates approximated by the normal modes. Arrows mark points of sudden energy exchange between the normal modes.

Phenomenology of OCS

What are these structures allowing transitions to other parts of phase space? In three dimensions, these invariant structures can be invariant tori with dimensions one (i.e. periodic orbits), two or three. These structures can also include the stable/unstable manifolds of these objects. How are invariant structures relevant in the phenomena of capture in chaotic systems? Since Hamiltonian systems do not possess “sinks”, no such dynamical object can attract and hold forever trajectories.

Phenomenology of OCS

Objects in Hamiltonian systems (such as equilibrium points, periodic orbits or invariant tori of various dimensions) according to their linear stability properties are “marginally stable” at best i.e. eigenvalues of their Jacobian matrix are unimodular. The only other qualitatively different behavior can be characterized as hyperbolic. Objects that are hyperbolic are characterized as saddle points: they both attract and repel, and typical trajectories passing by such objects are first slowed down as they approach it and then repelled as they move away from it.

Phenomenology of OCS

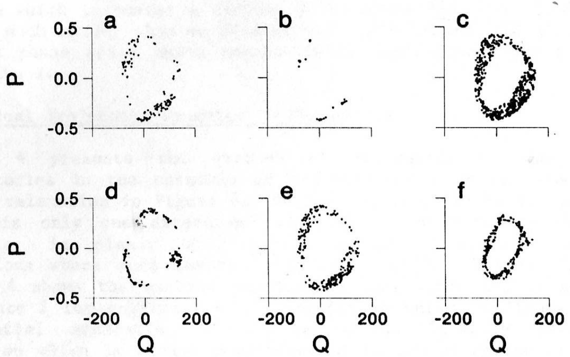

Figure 1. A series of time slices of a surface of section for a collinear OCS trajectory. The time ranges in ps of each plot are: a) 0.0 - 4.2, b) 4.2 - 7.0, c) 7.0 - 24.9, d) 24.9 - 30.0, e) 30.0 - 38.5, f) 38.5 - 45.3.

Phenomenology of OCS

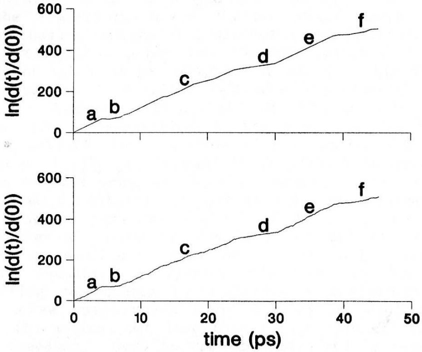

Figure 2. The bottom plot shows the ln of the relative distance between the collinear trajectory shown in Figure 1 and a collinear trajectory started initially very close to it. The top plot shows a 23 line fit to the bottom. The letters on these plots correspond to the plots in Figure 1.

Phenomenology of OCS

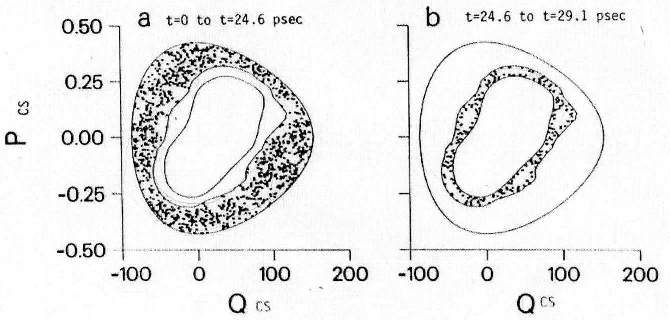

FIG. 2: (Q_{CS}, P_{CS}) surfaces of section for a collinear OCS trajectory. (a) First 24.6 ps of the trajectory. (b) Next 4.5 ps. Between (a) and (b), the trajectory crosses a phase space bottleneck.

Phenomenology of OCS

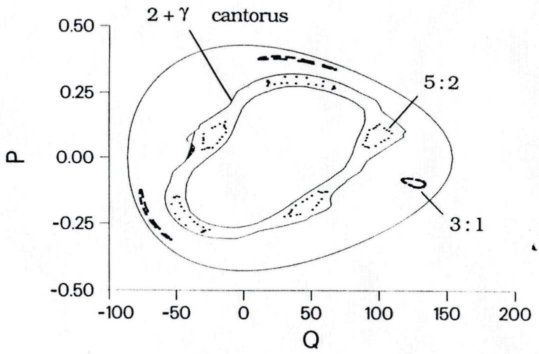

FIG. 3: Phase space structure of collinear OCS. Shown are the 3:1 and 5:2 resonance zones, and the $2+\gamma$ golden mean cantorus separating the two chaotic regions illustrated in Fig. 2.

Trapping and Roaming in 3d Hamiltonians

- Very slow relaxation; a “numerical experiment”:

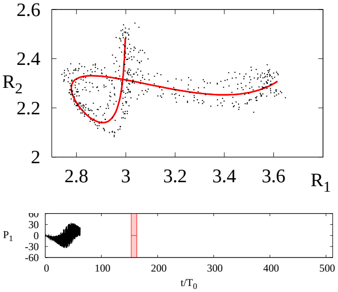

- Trapping stage
- Escape stage
- Chaos (or Roaming)

- Look for invariant surfaces
- 2-tori are important

Trapping and Roaming in 3d Hamiltonians

- Very slow relaxation; a “numerical experiment”:

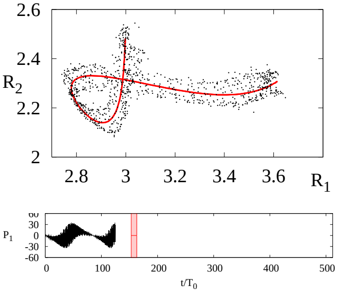

- Trapping stage
- Escape stage
- Chaos (or Roaming)

- Look for invariant surfaces
- 2-tori are important

Trapping and Roaming in 3d Hamiltonians

- Very slow relaxation; a “numerical experiment”:

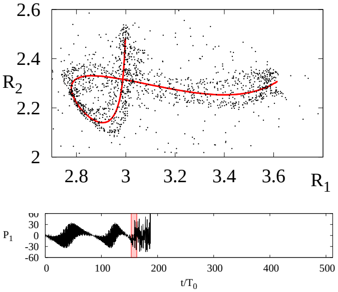

- Trapping stage
- Escape stage
- Chaos (or Roaming)

- Look for invariant surfaces
- 2-tori are important

Trapping and Roaming in 3d Hamiltonians

- Very slow relaxation; a “numerical experiment”:

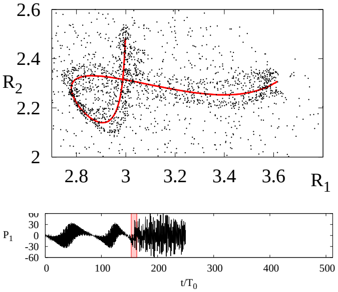

- Trapping stage
- Escape stage
- Chaos (or Roaming)

- Look for invariant surfaces
- 2-tori are important

Trapping and Roaming in 3d Hamiltonians

- Very slow relaxation; a “numerical experiment”:

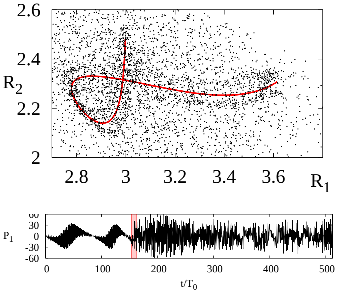

- Trapping stage
- Escape stage
- Chaos (or Roaming)

- Look for invariant surfaces
- 2-tori are important

Trapping and Roaming in 3d Hamiltonians

- Very slow relaxation; a “numerical experiment”:

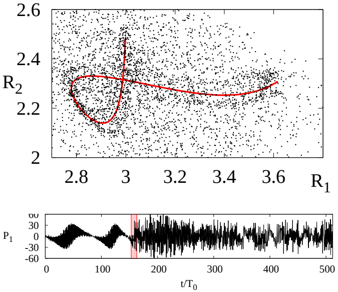

- Trapping stage
- Escape stage
- Chaos (or Roaming)

- Look for invariant surfaces
- 2-tori are important

Trapping and Roaming in 3d Hamiltonians

- Very slow relaxation; a “numerical experiment”:

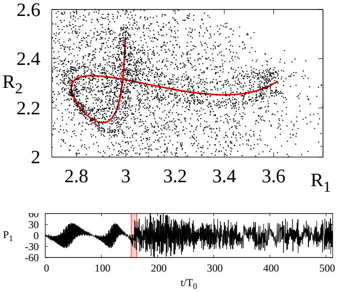

- Trapping stage
- Escape stage
- Chaos (or Roaming)

- Look for invariant surfaces
- 2-tori are important

"Stable" Periodic Orbits

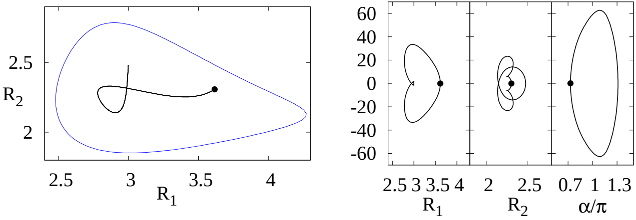

First we notice that if a trajectory is initiated along a periodic orbit, the system will never reach equilibrium since the energy will remain confined on the periodic orbit for all times. In the neighborhood of a periodic orbit, it is expected that, at least for a short time, the trajectory will mimic the dynamics of the periodic orbit (whatever its stability is) by continuity. After this *trapping* time, the trajectory might explore a larger domain in phase space.

Outline of the talk

Hydrogen atom in magnetic and electric fields: chaos.

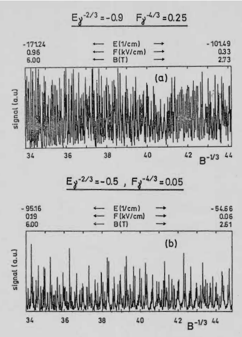

Hydrogen atom in magnetic and electric fields: chaos.

$$H = \frac{1}{2}\left(p_x - \frac{By}{2}\right)^2 + \frac{1}{2}\left(p_y + \frac{Bx}{2}\right)^2 + \frac{p_z^2}{2} + Fx - \frac{1}{\sqrt{x^2+y^2+z^2}}$$

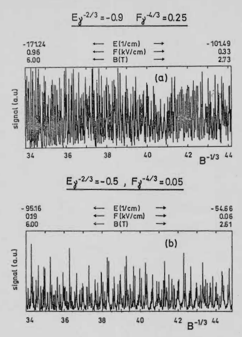

Hydrogen atom in magnetic and electric fields: chaos.

$$H = \frac{p_x^2 + p_y^2}{2} + B\frac{xp_y - yp_x}{2} + B^2\frac{x^2+y^2}{8} + Fx - 1/r$$

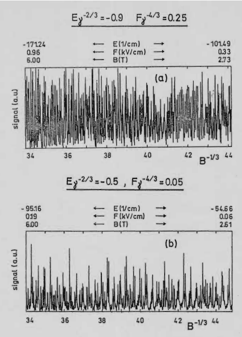

- $z = p_z = 0$
- $H = -0.8$, $F = 0.20661157$, $B = 1$
- Energy (far) above the threshold energy;
- Hard chaos, lots of UPOs;

Trapping by unstable orbits

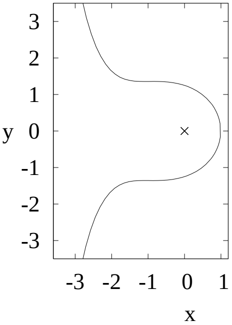

- Capture
- Trapping
- Escape
- Shadowing by unstable POs
- “Bottleneck” as an unstable PO

Trapping by unstable orbits

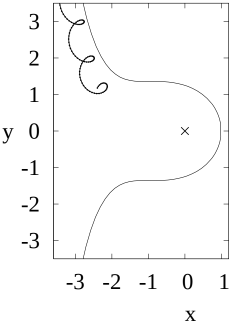

- Capture
- Trapping
- Escape
- Shadowing by unstable POs
- "Bottleneck" as an unstable PO

Trapping by unstable orbits

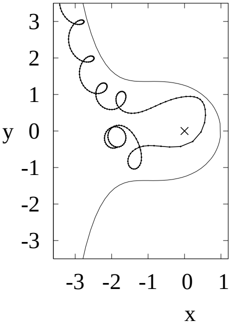

- Capture
- Trapping
- Escape
- Shadowing by unstable POs
- “Bottleneck” as an unstable PO

Trapping by unstable orbits

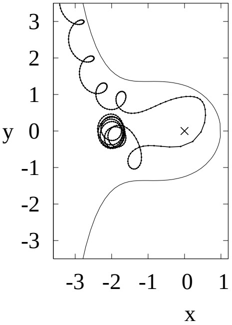

- Capture
- Trapping
- Escape
- Shadowing by unstable POs
- “Bottleneck” as an unstable PO

Trapping by unstable orbits

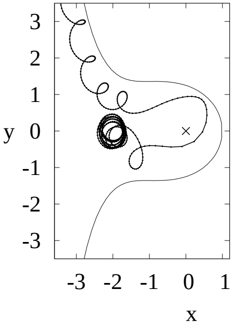

- Capture
- Trapping
- Escape
- Shadowing by unstable POs
- “Bottleneck” as an unstable PO

Trapping by unstable orbits

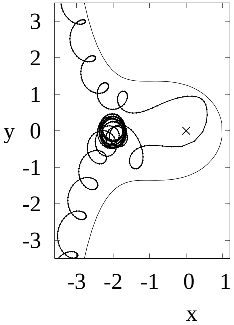

- Capture
- Trapping
- Escape
- Shadowing by unstable POs
- “Bottleneck” as an unstable PO

Trapping by unstable orbits

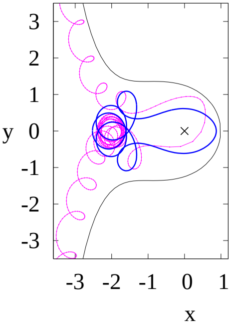

- Capture
- Trapping
- Escape
- Shadowing by unstable POs
- “Bottleneck” as an unstable PO

Trapping by unstable orbits

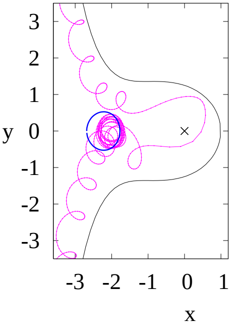

- Capture
- Trapping
- Escape
- Shadowing by unstable POs
- “Bottleneck” as an unstable PO

Outline of the talk

The Focus: Bottlenecks in OCS

- Planar carbonyl sulfide (OCS): a three degree of freedom Hamiltonian system, with no apparent symmetries, no small parameter ϵ, no possibility to estimate size of resonance zones.
- Mapping out resonance channels by invariant tori (on the surface of section), to explain energy transfer processes

The Focus: Bottlenecks in OCS

- Planar carbonyl sulfide (OCS): a three degree of freedom Hamiltonian system, with no apparent symmetries, no small parameter ϵ, no possibility to estimate size of resonance zones.
- Mapping out resonance channels by invariant tori (on the surface of section), to explain energy transfer processes

The Hamiltonian of a Rotationless OCS

$R_1, R_2, \alpha, P_1, P_2, P_\alpha$. $R_3 = \sqrt{R_1^2 + R_2^2 - 2R_1R_2\cos\alpha}$

$$H = T(R_1, R_2, \alpha, P_1, P_2, P_\alpha) + V(R_1, R_2, \alpha)\,,$$

$$\begin{aligned} T &= \frac{\mu_1 P_1^2}{2} + \frac{\mu_2 P_2^2}{2} + \mu_3 P_1 P_2 \cos\alpha - \mu_3 P_\alpha \sin\alpha \left(\frac{P_1}{R_2} + \frac{P_2}{R_1}\right) \\ &\quad + P_\alpha^2 \left(\frac{\mu_1}{2R_1^2} + \frac{\mu_2}{2R_2^2} - \frac{\mu_3 \cos\alpha}{R_1 R_2}\right) \end{aligned}$$

The Hamiltonian of a Rotationless OCS

$$V(R_1, R_2, \alpha) = \sum_{i=1}^{3} V_i(R_i) + V_I(R_1, R_2, R_3),$$

$$V_i(R_i) = D_i \left(1 - e^{-\beta_i \Delta R_i}\right)^2, \ \Delta R_i = (R_i - R_i^0) \qquad \text{Morse},$$

$$V_I = P(R_1, R_2, R_3) \prod_{i=1}^{3} (1 - \tanh \gamma_i \Delta R_i) \text{ Sorbie-Murrell},$$

$$\begin{aligned} P \quad = \quad & \sum (c_i \Delta R_i + c_{ij} \Delta R_i \Delta R_j + c_{ijk} \Delta R_i \Delta R_j \Delta R_k \\ & + c_{ijkl} \Delta R_i \Delta R_j \Delta R_k \Delta R_l) \text{ a quartic polynomial.} \end{aligned}$$

The Hamiltonian of a Rotationless OCS

Parameters:

- $A, D_i, R_i^0, \beta_i, \alpha_i, \gamma_i, c_i, c_{ij}, c_{ijk}$ $(i = 1, 2, 3)$ – fixed;
- $E = H(R_1, R_2, \alpha, P_1, P_2, P_\alpha)$ – tunable.

Collinear OCS ($\alpha = \pi$, $P_\alpha = 0$) equipotential lines:

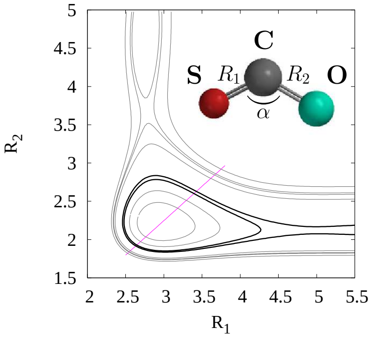

- Dissociation $E = 0.1$
- $E = 0.09 - 0.10$
- Chaotic

Transport theories

2-d:

- Tori – barriers $\rightarrow$ less volume partakes in transport.
  - γ tori – last destroyed by perturbations
- "small separatrix splitting" $\rightarrow$ power laws.

Ergodicity?

$(N \geq 3)$-d, chaotic.

- No barriers.
- Vanishing measure of N-tori (Froeschlé's conjecture.)

Transport theories

2-d:

- Tori – barriers $\rightarrow$ less volume partakes in transport.
  - γ tori – last destroyed by perturbations
- "small separatrix splitting" $\rightarrow$ power laws.

Ergodicity?

$(N \geq 3)$-d, chaotic.

- No barriers.
- Vanishing measure of N-tori (Froeschlé's conjecture.)

Transport theories

2-d:

- Tori – barriers $\rightarrow$ less volume partakes in transport.
  - γ tori – last destroyed by perturbations
- "small separatrix splitting" $\rightarrow$ power laws.

Ergodicity?

$(N \geq 3)$-d, chaotic.

- No barriers.
- Vanishing measure of N-tori (Froeschlé's conjecture.)

Outline of the talk

The Stability Landscape in Terms of Periodic Orbits

Define surface of section Σ to be the set of points $\mathbf{x}$ of a trajectory such that

$$U(\mathbf{x}) = 0\,,$$

with $\dot{\mathbf{x}} \cdot \partial U/\partial \mathbf{x} > 0$. From two consecutive points $\mathbf{x}_n = \mathbf{x}(t_n)$ and $\mathbf{x}_{n+1} = \mathbf{x}(t_n + \Delta(\mathbf{x}_n, t_n))$ on the Poincaré section, we define a *Poincaré map* $\mathcal{F}_\Sigma$,

$$\mathcal{F}_\Sigma(\mathbf{x}_n) = \mathbf{x}_{n+1}\,.$$

In what follows, we have used the surface Σ defined by

$$U(\mathbf{x}) = P_\alpha\,.$$

Periodic orbit is a fixed point on the surface of section, such that

$$\mathcal{F}^k_\Sigma(\mathbf{x}) = \mathbf{x}$$

The Stability Landscape in Terms of Periodic Orbits

Averaged density of periodic orbit points, projected onto the (R_1, R_2)-plane, weighted by the "local escape rate" γ_p^+, given by the sum of positive Lyapunov exponents, $\lambda_i^{(p)} > 0$ or, in terms of Lyapunov multipliers for the periodic orbit p, given by $\gamma_p^+ = \prod_{i:|\Lambda_i^{(p)}|\geq 1} |\Lambda_i^{(p)}|^{-1/T^{(p)}}$ where $\Lambda_i^{(p)}$ is an eigenvalue of $D\mathcal{F}_\Sigma$ evaluated at the periodic points. Periodic orbits with the following number of intersections with the Poincaré section are determined: $1(4)$, $2(9)$, $3(10)$, $5(24)$, $7(26)$, $11(40)$, $13(33)$, $17(21)$, $19(43)$, $23(41)$, $29(34)$, $31(28)$, $37(43)$, $8(101)$ where the number of orbits is shown in parentheses. Energy is set at $E = 0.09$. Lighter areas are dominated by more regular orbits, darker by unstable orbits. We analyze the region located near $\mathcal{O}_a$ where $(R_1, R_2) \approx (2, 2.5)$.

The Stability Landscape in Terms of Periodic Orbits

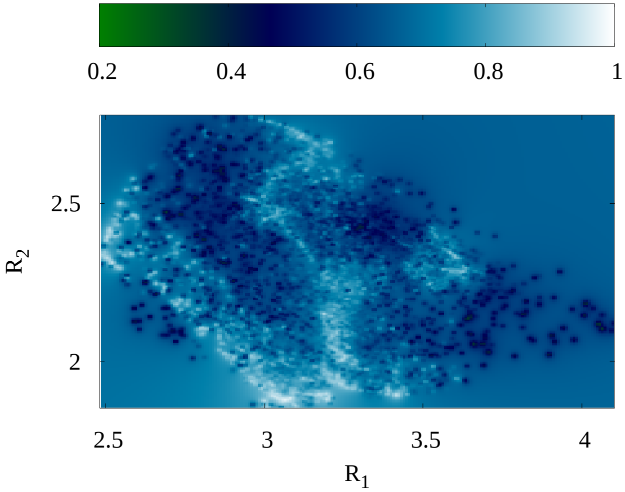

The Stability Landscape in Terms of Periodic Orbits

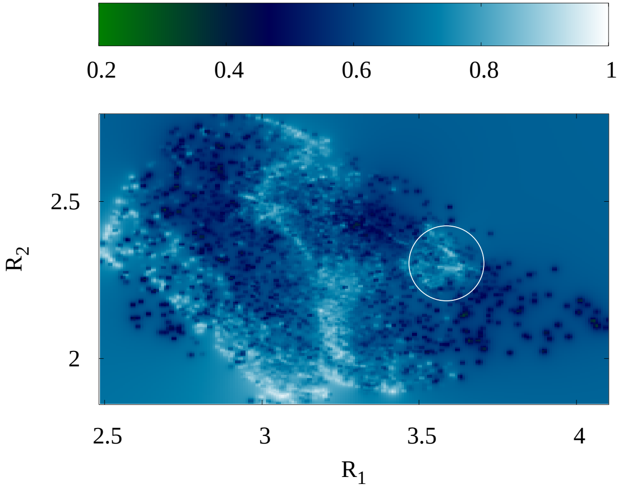

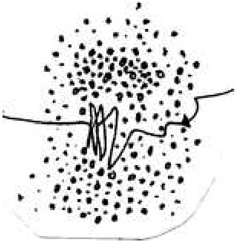

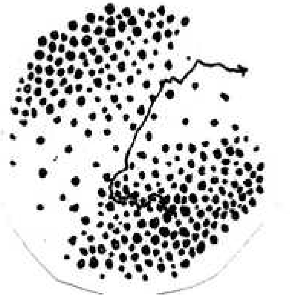

Temporal features: The Time-Frequency Analysis

A finite segment of a trajectory: $\{\mathbf{x}_n\}_{n=1,\dots,N}$, $\mathbf{x}_n = \mathbf{x}(t_n)$. Take snapshots with a fixed time increment, $t_{n+1} = t_n + \Delta$. To select only the main frequency, scale the time increment Δ by the period T_p of the organizing periodic orbit and select $\Delta = T_p/4$

Instantaneous frequencies: The Wavelet Decomposition

$$Wf(t,s) = \frac{1}{\sqrt{s}} \int_{-\infty}^{+\infty} f(\tau)\psi^* \left(\frac{\tau - t}{s}\right) d\tau \,. \tag{1}$$

Morlet-Grossman Wavelet (adjustable η and σ):

$$\psi(t) = e^{\iota\eta t} e^{-t^2/2\sigma^2}/(\sigma^2\pi)^{1/4} \tag{2}$$

Density of Energy in the time-frequency plane:

$$P_W f(t, \xi = \eta/s) = |Wf(t,s)|^2/s \,, \tag{3}$$

Ridges of P_W can be interpreted as instantaneous frequencies.

Instantaneous Frequencies: Trapping, Escape, Roaming.

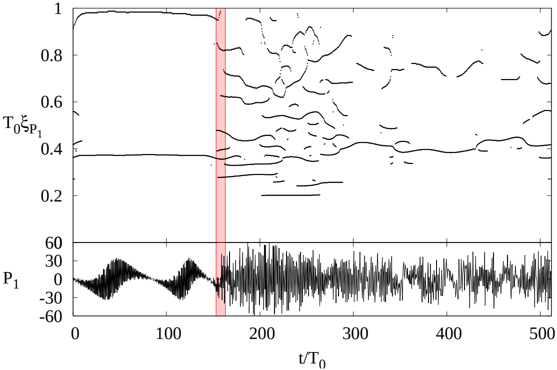

Instantaneous Frequencies: Trapping, Escape, Roaming.

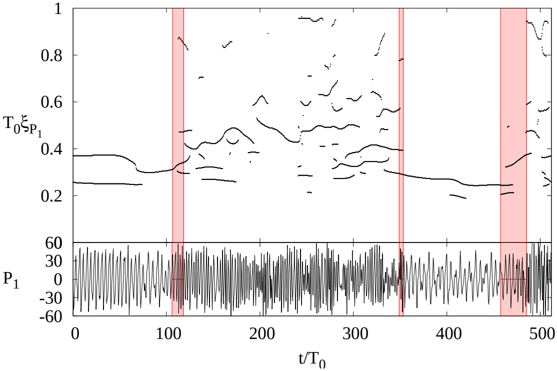

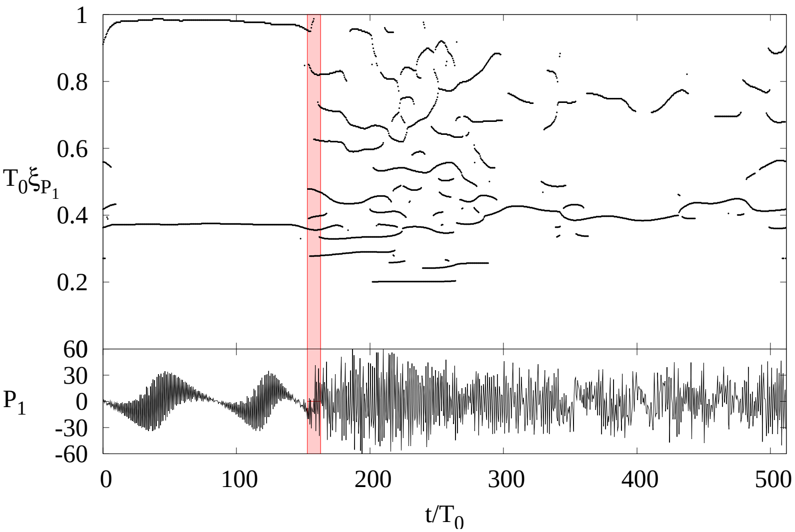
1
0.8
0.6
$T_0\xi_{P_1}$
0.4
0.2
60
30
0
-30
-60
P_1
0
100
200
300
400
500
t/T_0

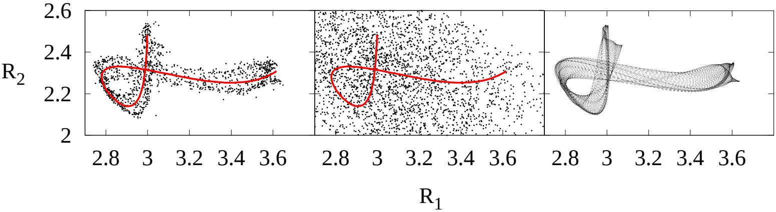
2.6
2.4
R_2
2.2
2
2.8
3
3.2
3.4
3.6
R_1

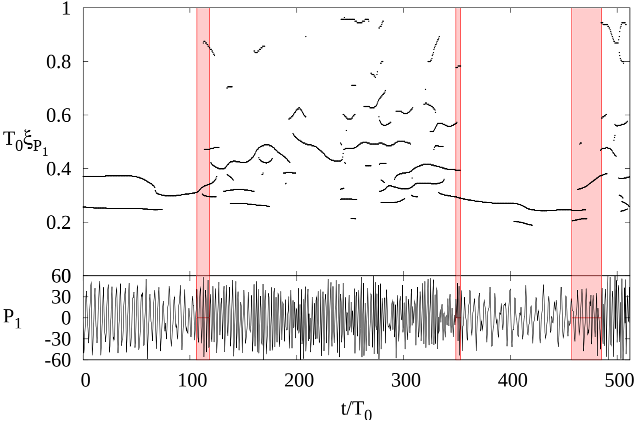
1
0.8
0.6
0.4
0.2
$T_0\xi_{P_1}$
60
30
0
-30
-60
P_1
0
100
200
300
400
500
t/T_0

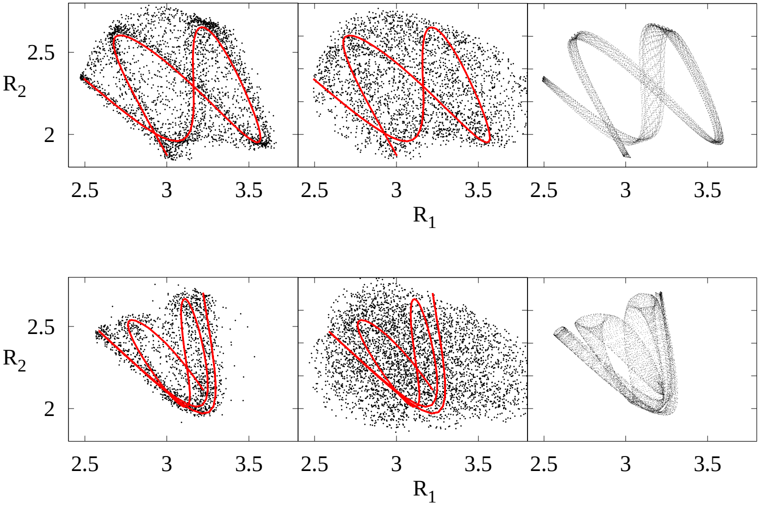
2.5
2
R2
2.5
3
3.5
R1

Trapping is Generic

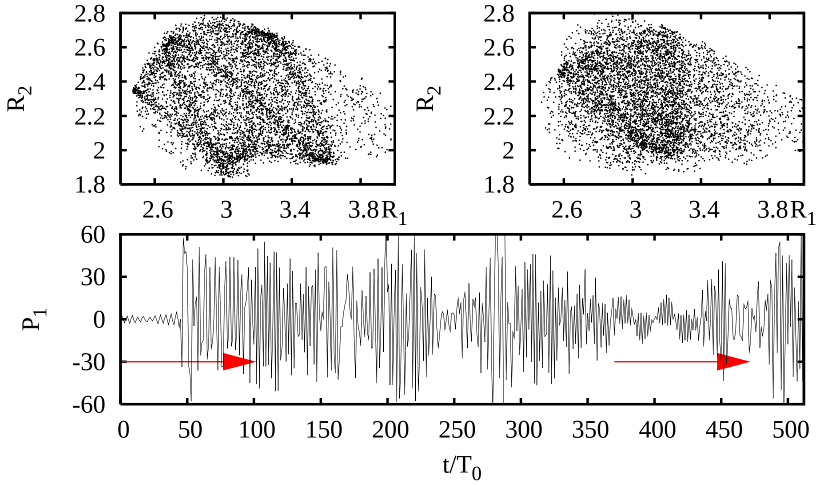

Outline of the talk

3-dof: Compact Invariant Surfaces

- Equilibria (0-dim)
- Periodic sausages (1-dim)
- two-dimensional sausages (2-dim)
- 3 dimensional sausages
- Normally Hyperbolic Invariant Würst

Continuation Procedure

Consider a fixed point $\mathbf{x}_0$ on the surface of section Σ, i.e. $\mathcal{F}_\Sigma(\mathbf{x}_0) = \mathbf{x}_0$. Near $\mathbf{x}_0$,

$$\mathcal{F}_\Sigma(\mathbf{x}) = \mathcal{F}_\Sigma(\mathbf{x}_0) + D\mathcal{F}_\Sigma(\mathbf{x}_0)(\mathbf{x} - \mathbf{x}_0) + \mathcal{R}(\mathbf{x} - \mathbf{x}_0)\,, \tag{4}$$

Consider a closed curve $\boldsymbol{\gamma}(s)$ on the Poincaré section Σ defined on a torus $s \in \mathbb{T}^1$, and consider the dynamics of $\mathbf{x}(s) = \mathbf{x}_0 + \epsilon\boldsymbol{\gamma}(s)$. If $D\mathcal{F}_\Sigma(\mathbf{x}_0)$ has at least one pair of eigenvalues in the form $\Lambda = \exp\left(\pm\imath\omega\right)$, it is possible to find a $\boldsymbol{\gamma}(s)$ such that $D\mathcal{F}_\Sigma\boldsymbol{\gamma}(s) = \boldsymbol{\gamma}(s + \omega_\epsilon)$ and $|\omega - \omega_\epsilon| = o(\epsilon)$. Therefore the equation

$$\mathcal{F}_\Sigma(\mathbf{x}(s)) = \mathbf{x}(s + \omega), \tag{5}$$

has a family of solutions, parametrized by the rotation number ω.

Computation of 2-d tori

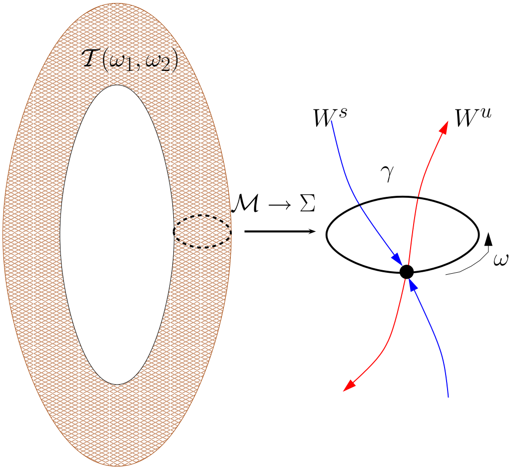

Project $\mathcal{M} \to \Sigma$

Loop $\gamma(\theta) = \gamma(\theta + 1)$

Rotation number ω

The type of internal dynamics on $\mathbb{T}^1$ is likely to be a rotation. We assume that the Poincaré map $\mathcal{F}_\Sigma$ has an invariant curve with an irrational rotation number ω, and that there exists a map (at least continuous) $\mathbf{x} : \mathbb{T}^1 \mapsto \Sigma$ such that a *rotation number* ω can be defined.

$$\mathbf{F}(\mathbf{x})(\theta) = \mathcal{F}_\Sigma(\mathbf{x}(\theta)) - (T_\omega \mathbf{x})(\theta). \tag{6}$$

The zeros of $\mathbf{F}$ correspond to (continuous) invariant curves of rotation number ω.

First we expand $\mathbf{x}(\theta)$ in a Fourier series with real coefficients,

$$\mathbf{x}(\theta) = \frac{\mathbf{a}_0}{2} + \sum_{k>0} \left(\mathbf{a}_k \cos \pi k\theta + \mathbf{b}_k \sin \pi k\theta\right), \qquad (7)$$

where $\mathbf{a}_k, \mathbf{b}_k \in \mathbb{R}^n$ for $k \in \mathbb{N}$ (n being the dimension of the flow) and $\mathbf{x}(\theta)$ is a periodic function with period 2, i.e. $\mathbf{x}(\theta + 2) = \mathbf{x}(\theta)$.
Truncate these series at a fixed value of N, $2N + 1$ unknown coefficients $\mathbf{a}_0$, $\mathbf{a}_k$, and $\mathbf{b}_k$ for $1 \leq k \leq N$. A mesh of $2N + 1$ points on $\mathbb{T}^1$:

$$\theta_j = \frac{2j}{2N+1} \quad \text{for } 0 \leq j \leq 2N,$$

$\mathcal{F}_\Sigma(\mathbf{x}(\theta_j))$ are functions of $\mathbf{a}_k$, $\mathbf{b}_k$:

$$\begin{aligned}\mathbf{F}_j(\{\mathbf{a}_k\},\{\mathbf{b}_k\},\omega) &= \mathcal{F}_\Sigma(\phi(\{\mathbf{a}_k\},\{\mathbf{b}_k\},j)) \\ &\quad -\phi(\{\mathbf{a}_k\},\{\mathbf{b}_k\},j+i(\omega)),\end{aligned}$$

for $0 \le j \le 2N$ and where $i(\omega) = (2N+1)\omega/2$, and $\mathbf{a}_k$s, $\mathbf{b}_k$s are the unknowns in the above equation.

$$\mathbf{F}_j(\mathbf{a},\mathbf{b},\nu) + \frac{\partial \mathbf{F}_j}{\partial \mathbf{a}_k}\delta\mathbf{a}_k + \frac{\partial \mathbf{F}_j}{\partial \mathbf{b}_k}\delta\mathbf{b}_k + \frac{\partial \mathbf{F}_j}{\partial \omega}\delta\omega = 0\,,$$

where $\mathbf{a} = (\mathbf{a}_0, \mathbf{a}_1, \ldots, \mathbf{a}_N)$ and $\mathbf{b} = (\mathbf{b}_1, \ldots, \mathbf{b}_N)$. If $\mathbf{x}(\theta)$ is a Fourier series corresponding to an invariant curve then, for any $\varphi \in \mathbb{T}^1$, $\mathbf{y}(\theta) \equiv \mathbf{x}(\theta+\varphi)$ is a different Fourier series corresponding to the same invariant curve as $\mathbf{x}(\theta)$. The Jacobian of $\mathbf{F}_j$ around the invariant curve has, at least, a one-dimensional kernel. Use the SVD.
Testing the spectrum of the solution (and the norm of its eigenvectors weighted by the frequency, penalizing high harmonics): a smooth solution should contain a unit eigenvalue.

Normal stability

Normal stability properties of invariant loops are determined by the solutions (Λ,ψ) of the generalized eigenvalue problem,

$$D\mathcal{F}_{\Sigma}(x)(\theta)\psi(\theta) = \Lambda T_{\omega}\psi(\theta)\,,$$

The eigenvalues Λ have the following properties: 1) $\Lambda = 1$ is an eigenvalue; the corresponding eigenvector is the derivative of the loop $\mathbf{x}$, 2) if Λ is an eigenvalue; then $\Lambda \exp\left(2\imath k\pi\omega\right)$ is also an eigenvalue for any $k \in \mathbb{Z}$, 3) the closure of the set of eigenvalues is a union of circles centered at the origin.

Accuracy of eigenvalues can be estimated by

$$\|\psi\|^{(p)} = \sum_j |\psi_i||j|^p$$

Normal stability

Normal stability properties of invariant loops are determined by the solutions (Λ,ψ) of the generalized eigenvalue problem,

$$D\mathcal{F}_{\Sigma}(x)(\theta)\psi(\theta) = \Lambda T_{\omega}\psi(\theta)\,,$$

The eigenvalues Λ have the following properties: 1) $\Lambda = 1$ is an eigenvalue; the corresponding eigenvector is the derivative of the loop $\mathbf{x}$, 2) if Λ is an eigenvalue; then $\Lambda \exp\left(2\iota k\pi\omega\right)$ is also an eigenvalue for any $k \in \mathbb{Z}$, 3) the closure of the set of eigenvalues is a union of circles centered at the origin.

Accuracy of eigenvalues can be estimated by

$$\|\psi\|^{(p)} = \sum_j |\psi_i||j|^p$$

Jacobian Projection in Local Coordinates

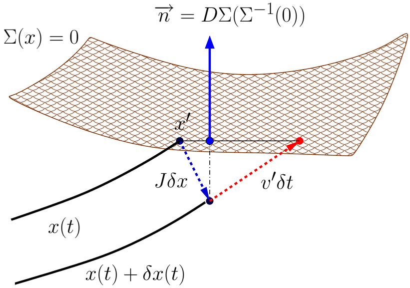

Figure: Reduction of the Jacobian $D\mathcal{F}_\Sigma(x, \tau)$ to derivative of the map $D\mathcal{F}_\Sigma(x)$. If $x(t)$ intersects the Poincaré section at $x' \in \Sigma$ at time τ, the nearby $x(t) + \delta x(t)$ trajectory intersects it time $\tau + \delta t$ later. As $(\overrightarrow{n} \cdot v'\delta t) = -(\overrightarrow{n} \cdot D\mathcal{F}_\Sigma\, \delta x)$, the difference in arrival times is given by $\delta t = -(\overrightarrow{n} \cdot D\mathcal{F}_\Sigma\, \delta x)/(\overrightarrow{n} \cdot v')$, and the projection of the Jacobian to the surface of section is $D\mathcal{F}_\Sigma(x_0) \simeq D\tilde{\mathcal{F}}_{\Sigma ij} = D\mathcal{F}_{\Sigma ij} - v'_i(\overrightarrow{n} \cdot D\mathcal{F}_\Sigma)_j/(\overrightarrow{n} \cdot v')$.

If (X, Ω) and (Y, Ξ) are symplectic vector spaces, a smooth map $f : X \mapsto Y$ is called symplectic (canonical) if it preserves the symplectic (canonical) forms, that is, if

$$\Xi(\mathbf{D}f(z) \cdot z_1, \mathbf{D}f(z) \cdot z_2) = \Omega(z_1, z_2)$$

$$(\mathbf{P}(u, v))_{ij} = \mathbf{1}_{ij} - \frac{u_i v_j}{\langle v, u \rangle} \tag{8}$$

The normal vector to the co-dimension-one surface of section is $n(x)$, $x \in \Sigma$. The surface of section maps $x' = \mathcal{F}_\Sigma(x)$. We denote derivative of the Hamiltonian as a vector by $h(x) = \mathbf{d}H(x)$, and $h = h(x)$, $h' = h(x')$, and similarly $v = v(x)$, $v' = v(x')$. We also denote $\tilde{n}(x) = \mathbb{I}n(x)$.

$$\tilde{\mathbf{J}} = \mathbf{P}(v(x'), n(x'))\mathbf{J}\mathbf{P}(\mathbb{I}n(x), \mathbb{I}v(x)) \tag{9}$$

In practice locally Σ is defined by $x_m = 0 : n(x)_i = \delta_{im}$, $(\mathbb{I}n(x))_i = \delta_{i\sigma(m)}$, $\sigma(m)$ is the index of the canonically conjugate variable to x_m.

Poincaré Surface of Section

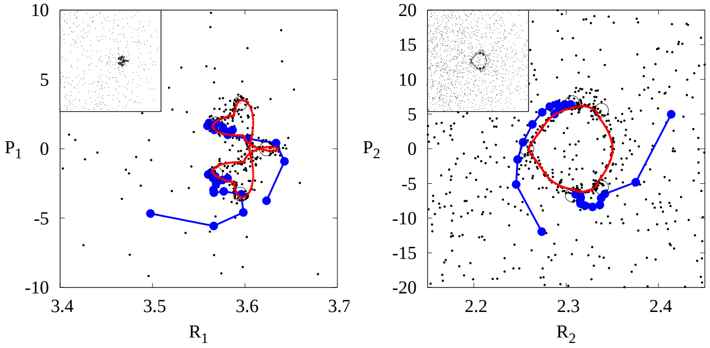

Poincaré Surface of Section

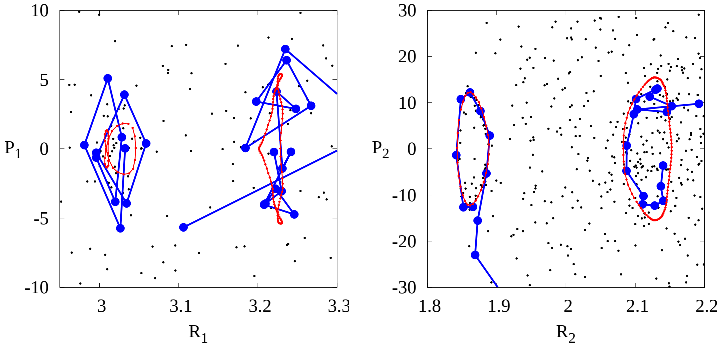

Frequency-Halving Bifurcation

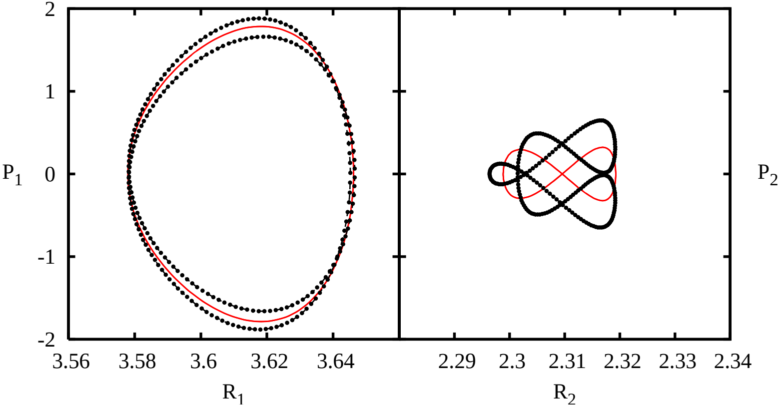

Mechanism of Capture in The Resonance

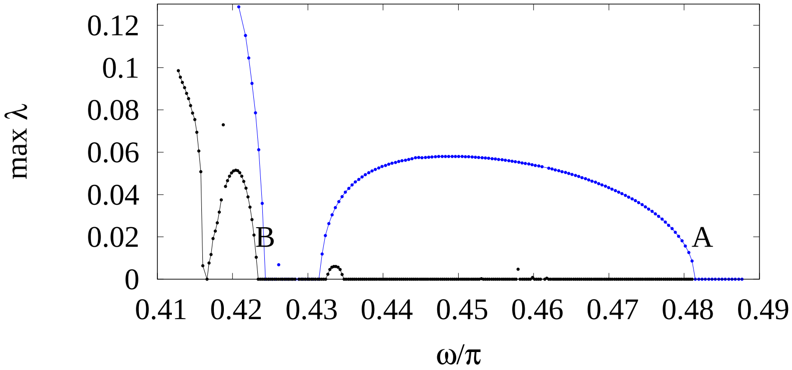

Mechanism of Capture in The Resonance

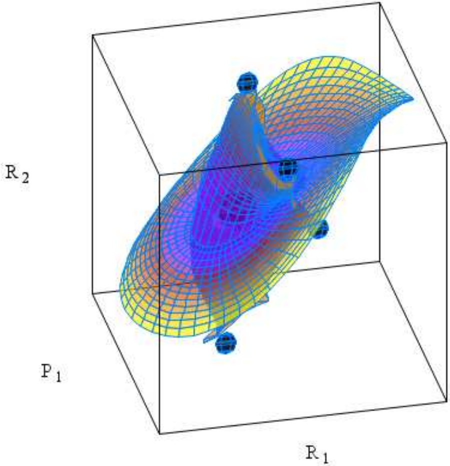

Outline of the talk

1. Observations and Phenomenology of Energy Transfer Processes
   - Transfer of Energy in Small Molecules
   - Chaotic transport: Hydrogen in Crossed Fields
   - Summary

2. Focus: Invariant Tori in the Phase Space of OCS
   - Tools to Detect Resonances
   - Unstable Tori as Transition Bottlenecks
   - Geometry of Invariant Surfaces

Normally Non-Hyperbolic Invariant Manifolds

Rational Rotation Numbers

Bifurcations, complicated configurations happen because these surfaces are *not* Normally Hyperbolic.

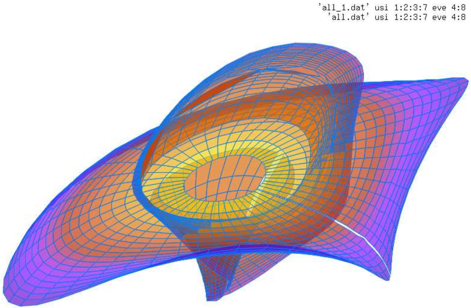

Normally Non-Hyperbolic Invariant Manifolds

Rational Rotation Numbers

Bifurcations, complicated configurations happen because these surfaces are *not* Normally Hyperbolic.

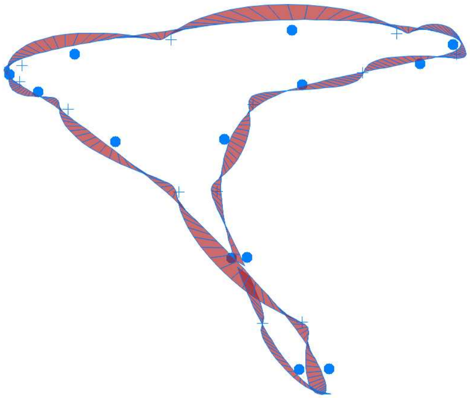

Normally Non-Hyperbolic Invariant Manifolds

Rational Rotation Numbers

Bifurcations, complicated configurations happen because these surfaces are *not* Normally Hyperbolic.

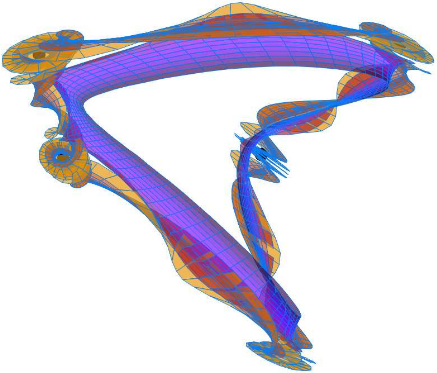

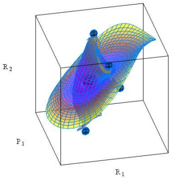

Normally Non-Hyperbolic Invariant Manifolds

Rational Rotation Numbers

Bifurcations, complicated configurations happen because these surfaces are *not* Normally Hyperbolic.

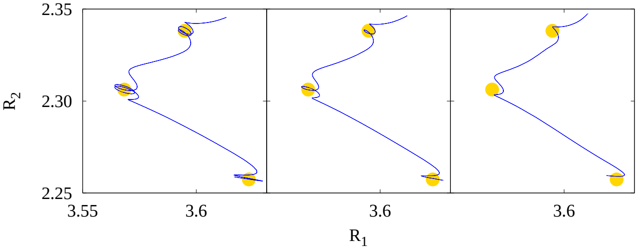

Summary

- Crossover between trapping and Roaming of trajectories has been identified as transition from a resonance channel to chaotic zone (and vice versa.)
- Codimension-one invariant tori can be used to map out the resonance channels, and their bifurcations to identify points of transition.

R. Paškauskas, C. Chandre, and T. Uzer, *Phys. Rev. Lett.*, **100**, 083001, 2008.

Summary

- Crossover between trapping and Roaming of trajectories has been identified as transition from a resonance channel to chaotic zone (and vice versa.)
- Codimension-one invariant tori can be used to map out the resonance channels, and their bifurcations to identify points of transition.

R. Paškauskas, C. Chandre, and T. Uzer, *Phys. Rev. Lett.*, **100**, 083001, 2008.

Outlook

A challenging problem: Many body systems with Long-Range Interactions. Applications in plasma physics.

- Large number of degrees of freedom ($N \sim 10^{3-6}$)
- Energy transfer to the Thermodynamic Mode occurs on a very slow time scale, $t \sim N^{1+\gamma}$. Is it due to resonances?